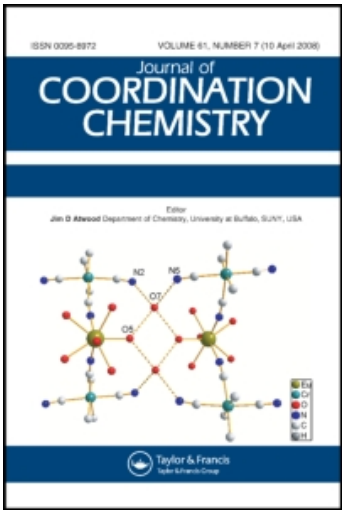

Journal of Coordination Chemistry
Publication details, including instructions for authors and subscription information:
http://www.informaworld.com/smpp/title~content=t713455674

Group 12 metal(II) complexes with 1-methylimidazoline-2(3*H*)-thione (mitH): correlation between crystal structure and physicochemical property

Yuki Matsunaga[a]; Kiyoshi Fujisawa[a]; Nagina Amir[a]; Yoshitaro Miyashita[a]; Ken-Ichi Okamoto[a]
[a] Department of Chemistry, University of Tsukuba, Tsukuba 305-8571, Japan

To cite this Article Matsunaga, Yuki , Fujisawa, Kiyoshi , Amir, Nagina , Miyashita, Yoshitaro and Okamoto, Ken-Ichi(2005) 'Group 12 metal(II) complexes with 1-methylimidazoline-2(3*H*)-thione (mitH): correlation between crystal structure and physicochemical property', Journal of Coordination Chemistry, 58: 12, 1047 — 1061
To link to this Article: DOI: 10.1080/00958970500122524
URL: http://dx.doi.org/10.1080/00958970500122524

Journal of Coordination Chemistry
Vol. 58, No. 12, 15 August 2005, 1047–1061

Group 12 metal(II) complexes with 1-methylimidazoline-2(3*H*)-thione (mitH): correlation between crystal structure and physicochemical property

YUKI MATSUNAGA, KIYOSHI FUJISAWA*, NAGINA AMIR, YOSHITARO MIYASHITA and KEN-ICHI OKAMOTO

Department of Chemistry, University of Tsukuba, Tsukuba 305-8571, Japan

(*Received 23 April 2004; revised 26 October 2004; in final form 31 March 2005*)

The crystal structures of $[ZnX_2(mitH)_2]$ (X = Cl (**1**), Br (**2**)), $[ZnI(mitH)_3]I$ (**3**), and $[CdX_2(mitH)_2]$ (X = Cl (**4**), Br (**5**), I (**6**)) (mitH = 1-methylimizadoline-2(3*H*)-thione) were determined by X-ray crystallography and all complexes were characterized by IR, far-IR, Raman, and UV–Vis absorption (solid) spectroscopies. All complexes except **3**, which have a different $ZnIS_3$ coordination mode, have a distorted tetrahedral geometry with an MX_2S_2 coordination mode. Each π-character of the C=S bonds (from 37.7 to 45.4%) is smaller than that of free mitH (51.9%). Their M–S–C bond angles (from 97° to 109°) support that the C=S bonds are not a full double bond. Their stretching vibration frequencies of M–S (300–320 cm^{-1}) and M–X (229–290 cm^{-1}) in both far-IR and Raman spectra show the lower energy shifts with increasing weight of metal(II) or halide ions. Similarly, some shifts (from 275 nm for **1** to 293 nm for **6**) are also observed in CT transition bands in UV-Vis absorption spectra.

Keywords: Crystal structure; Zinc(II); Cadmium(II); Thione complexes

1. Introduction

Zinc is one of the minor elements *in vivo*. It has a variety of structural types, which have been defined by X-ray analysis in living systems [1]. One ZnN_2S_2 type is found in the zinc finger in biological systems. These structures of Zn(II) sites have in common a +II oxidation state and a four-coordinate, tetrahedral geometry. These Zn(II) sites are formed by their side chains of Cys (S donor), His (N donor), and occasionally Asp or Glu (O donor). In order to study their structural and physicochemical properties, many model complexes have been reported so far [2–6].

Cadmium and mercury have severe toxicity in the body. In order to shed light on their detoxification mechanisms, coordination chemistry containing these metals and the sulfur atoms is now a current topic in inorganic and bioinorganic chemistry [7]. In particular, a mercury detoxification mechanism has been only

*Corresponding author. Fax: +81-29-853-6503. Tel.: +81-29-853-6922. Email: kiyoshif@chem.tsukuba.ac.jp

Journal of Coordination Chemistry
ISSN 0095-8972 print: ISSN 1029-0389 online
DOI: 10.1080/00958970500122524

reported in a multifunctional regulatory protein, merR [8, 9]. The coordination number and donor atoms around Hg(II) ions in this protein were determined by spectroscopic methods such as UV absorption, ^{199}Hg-NMR, and EXAFS spectroscopies for merR in comparison with Hg(II) model complexes having a HgS_3 coordination mode, $[Hg(SBu^t)_3]^-$ [10–12]. From these results, it is clear that Hg(II) ion binds to the cysteine thiol group in three-coordinate fashion in merR and it indicates that model complexes are useful for this study.

Physicochemical studies for zinc model complexes should be useful for understanding the relationship between metal(II) ion and coordinated donor atoms such as merR. However, reports for spectroscopic characterizations of Zn(II) and Cd(II) complexes are a few. Most model complexes contain an aromatic ring in ligands, which contributes partially to complex stability by aromatic ring-sulfur interaction. These thiolato complexes containing d^{10} metal ions have some CT transitions. These transitions are overlapped with absorption band(s) arising from aromatic ring(s) of ligand(s). Consequently, these complexes are unsuitable for assignment of exact CT transition energies. In this study, 1-methylimidazoline-2(3*H*)-thione (mitH), which contains both sulfur and nitrogen donor atoms, is used in order to elucidate the stereochemistry and physicochemical properties of group 12 metal(II) model complexes containing sulfur donor atoms. The model complex with mitH ligand is suitable for assignment of its CT transition because the imidazole ring has weaker absorption bands than aromatic rings in the UV region. The mitH ligand is a versatile and unique ligand, capable of existing in thiol (C–SH) and thione (C=S) tautomeric forms as shown in equation (1) and has a variety of coordination geometries. Complexes with mitH have been known for Co(II) [13, 14], Ni(II) [15], Cu(I) [16–18], Zn(II) [14, 19], Ga(I) [20], Mo(II) [20], Cd(II) [14], Re(I) [20], and Hg(II) [21–24]. The ligand in these complexes mainly exists as a neutral ligand (thione form), and coordinates with an S donor atom. In 1983, Shunmugam and Sathyanarayana reported the synthesis and physicochemical properties of MX_2S_2 type complexes (M = Zn, Cd, Hg; X = Cl, Br), however, their structures have not been determined [25]. Recently, X-ray structures of Hg(II) complexes, ($[HgX_2(mitH)_2]$ (X = Cl, Br, I)), were reported, having a pseudo-tetrahedral geometry [21]. In this article, we report the synthesis, stereochemistry, and physicochemical properties of $[MX_2(mitH)_2]$ (M = Zn, X = Cl (**1**), Br (**2**); M = Cd, X = Cl (**4**), Br (**5**), I (**6**)) and $[ZnI(mitH)_3]I$ (**3**), on the basis of X-ray analysis, IR, far-IR, Raman, and UV-Vis (solid state) spectroscopies.

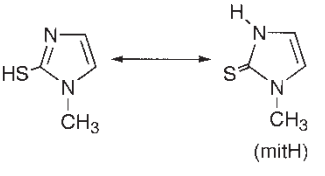

(1)

2. Experimental

2.1. *Materials and methods*

$ZnCl_2$, $ZnBr_2$, ZnI_2, $CdCl_2 \cdot 2.5H_2O$, $CdBr_2 \cdot 4H_2O$, and CdI_2 were obtained from Wako Pure Chemical Int. Ltd. 1-methylimidazoline-2(3*H*)-thione (mitH) was obtained

from Tokyo Kasei Kogyo Co., Ltd. They were used without further purification. $[HgCl_2(mitH)_2]$ was prepared according to the literature [21]. All the solvents were commercially available and used without further purification.

IR spectra and far-IR spectra were recorded using KBr pellets in the 4600–400 cm^{-1} region and CsI pellets in the 650–100 cm^{-1} region on a JASCO FT/IR-550 spectrophotometer. FT-Raman spectra were measured using KBr pellets in the 3500–100 cm^{-1} region on a Perkin-Elmer Spectrum GX spectrophotometer. UV-Vis absorption spectra of solution state were recorded in the 200–500 nm region on a JASCO V-570 spectrophotometer. UV-Vis absorption spectra in solid state were recorded using fine powder mull samples, which were prepared by finely grinding the solid materials, in the same region (200–500 nm) with a JASCO V-560 spectrophotometer. These were suspended in mineral oil (poly(dimethylsiloxane), Aldrich) and spread between quartz plates. Elemental analysis (C, H, N) was performed by the Chemical Analysis Center of the University of Tsukuba or the elemental analysis facility of our department.

2.2. *Preparation of $[ZnCl_2(mitH)_2]$ (1)*

To a CH_3OH solution (40 cm^3) of mitH (1.16 g, 10 mmol), a CH_3OH solution (5 cm^3) of $ZnCl_2$ (0.69 g, 5.0 mmol) was added. When the mixture was stirred for 1 h, a white solid appeared. The resulting white powder was collected by filtration and washed with CH_3OH. The colorless single crystals for X-ray analysis were obtained by cooling the filtrate for a few days in the refrigerator. These crystals were assigned to the same complex as the white powder by the physicochemical properties. Yield: 49% (0.89 g). Anal. Calcd for $C_8H_{12}N_4S_2ZnCl_2$ (%): C, 26.35; H, 3.31; N, 15.36. Found: C, 26.28; H, 3.40; N, 15.12. IR (cm^{-1}): 3251vs, 3136s, 3044w, 2945w, 1576vs, 1478vs, 1467vs, 1282m, 1254w, 1156m, 1087m, 748m, 732vs, 684m, 670s, 516m. Far-IR (cm^{-1}): 422w, 408m, 320s, 304s(sh), 290vs, 242s, 225w, 202w, 183w. FT-Raman (cm^{-1}): 3179w, 3135w, 3119w, 2947m, 1574w, 1478vs, 1455vs, 1350m, 1282s, 1254w, 1158w, 1090w, 922m, 689m, 518w, 422w, 317sh, 303w, 284m, 202w. (Symbols: vs, very strong; s, strong; m, medium; w, weak; sh, shoulder).

2.3. *Preparation of $[ZnBr_2(mitH)_2]$ (2)*

This complex was prepared by a similar procedure to **1** using $ZnBr_2$ (1.13 g, 5.0 mmol) and mitH (1.14 g, 10 mmol). Yield: 29% (0.67 g). The colorless single crystals for X-ray analysis were obtained by recrystallization of white powder from a CH_3OH/H_2O mixed solvent. Anal. Calcd for $C_8H_{12}N_4S_2ZnBr_2$ (%): C, 21.18; H, 2.66; N, 12.35. Found: C, 21.15; H, 2.65; N, 12.18. IR (cm^{-1}): 3204s, 3160m, 3130m, 2938w, 1573s, 1475vs, 1458vs, 1278m, 1142m, 1094w, 741s, 689m, 675m, 518w. Far-IR (cm^{-1}): 422w, 404m, 320s, 302s, 306m(sh), 242vs, 221vs, 196m, 177w. FT-Raman (cm^{-1}): 3166w, 3130m, 2946m, 1576w, 1449vs, 1351m, 1286m, 1258m, 1161w, 1099w, 920m, 689s, 516w, 314w, 301w, 253m, 196m.

2.4. *Preparation of $[ZnI(mitH)_3]I$ (3)*

The synthesis was carried out by the same method as **1** using ZnI_2 (1.60 g, 5.0 mmol) and mitH (1.14 g, 10 mmol). Yield: 43% (1.43 g). The colorless single crystals for X-ray analysis were obtained by cooling the filtrate for a few days in the refrigerator.

Anal. Calcd for $C_{12}H_{18}N_6S_3ZnI_2$ (%): C, 21.78; H, 2.74; N, 12.70. Found: C, 21.61; H, 2.78; N, 12.54. IR (cm^{-1}): 3282vs, 3119vs, 2943w, 1574vs, 1457vs, 1283s, 1158m, 1098s, 757s, 716s, 516w. Far-IR (cm^{-1}): 404s, 304m, 262m(sh), 237vs, 194s, 169w. FT-Raman (cm^{-1}): 3161w, 3120m, 2945m, 1576m, 1453vs, 1353m, 1284m, 1157m, 917m, 690s, 517m, 404w, 314w, 305sh, 236w, 193w.

2.5. *Preparation of [$CdCl_2(mitH)_2$] (4)*

The synthesis was carried out by the same method as **1** using $CdCl_2 \cdot 2.5H_2O$ (1.15 g, 5.0 mmol) and mitH (1.14 g, 10 mmol). Yield: 83% (1.71 g). The colorless single crystals for X-ray analysis were obtained by recrystallization from a CH_3OH/H_2O mixed solvent. Anal. Calcd for $C_8H_{12}N_4S_2CdCl_2$ (%): C, 23.34; H, 2.94; N, 13.61. Found: C, 23.12; H, 3.04; N, 13.51. IR (cm^{-1}): 3137vs, 3153vs, 3117vs, 3039m, 2944w, 1575s, 1479vs, 1288m, 1159m, 1103w, 754s, 729s, 665m, 512m. Far-IR (cm^{-1}): 420m, 306m, 271vs, 241s, 227m(sh), 213m, 183w, 167w. FT-Raman (cm^{-1}): 3175w, 3134m, 3117m, 2949m, 1580w, 1465vs, 1354m, 1291s, 1276w, 1157m, 920m, 691m, 603w, 511w, 420w, 303w, 294w, 272m, 238m, 189w.

2.6. *Preparation of [$CdBr_2(mitH)_2$] (5)*

The synthesis was carried out by the same method as **1** using $CdBr_2 \cdot 4H_2O$ (1.72 g, 5.0 mmol) and mitH (1.15 g, 10 mmol). Yield: 84% (2.11 g). The colorless single crystals for X-ray analysis were obtained by recrystallization from a CH_3OH/H_2O mixed solvent. Anal. Calcd for $C_8H_{12}N_4S_2CdBr_2$ (%): C, 19.19; H, 2.41; N, 11.19. Found: C, 19.08; H, 2.39; N, 10.92. IR (cm^{-1}): 3245vs, 3123s, 3039w, 2941w, 1576s, 1468s, 1287m, 1157m, 1101m, 736vs, 674s, 665m, 515w. Far-IR (cm^{-1}): 408m, 306m, 291w, 250m, 242m, 229s, 201w, 188m, 174vs, 163s(sh). FT-Raman (cm^{-1}): 3166w, 3127m, 2944m, 1575w, 1451vs, 1351m, 1285m, 1259m, 1160w, 1098w, 919m, 689m, 515w, 302w, 291w, 250m, 240w, 229w, 190m.

2.7. *Preparation of [$CdI_2(mitH)_2$] (6)*

The synthesis was carried out by the same method as **1** using CdI_2 (1.83 g, 5.0 mmol) and mitH (1.15 g, 10 mmol). Yield: 80% (2.37 g). The colorless single crystals for X-ray analysis were obtained by recrystallization from a CH_3OH/H_2O mixed solvent. Anal. Calcd for $C_8H_{12}N_4S_2CdI_2$ (%): C, 16.16; H, 2.03; N, 9.42. Found: C, 16.43; H, 2.00; N, 9.30. IR (cm^{-1}): 3270vs, 3165m, 3124s, 2939w, 1577vs, 1475vs, 1452s, 1284m, 1155m, 1099m, 731s, 670m, 656m, 514w. Far-IR (cm^{-1}): 415m, 406m, 300vs, 253w, 230vs, 186m. FT-Raman (cm^{-1}): 3167w, 3126m, 2941m, 1575m, 1449vs, 1351m, 1283m, 1254m, 1153w, 1100w, 919m, 687s, 514w, 414w, 292w, 254w, 228m, 221w, 187w.

2.8. *Crystal structure determination*

Crystal data and refinement parameters for **1–6** are given in table 1. The diffraction data for all complexes were measured on a Rigaku AFC7S automated four-circle diffractometer with graphite monochromated Mo Kα ($\lambda = 0.71069$ Å) radiation at room temperature for **1**, **3**, **4**, and **6** and at low temperature for **2** (−53 °C)

Table 1. Summary of crystallographic data of $[MX_2(mitH)_2]$ (M = Zn; X = Cl (**1**), Br (**2**), M = Cd; X = Cl (**4**), Br (**5**), I (**6**)) and $[ZnI(mitH)_3]I$ (**3**).

Empirical formula	$C_8H_{12}N_4S_2Cl_2Zn$	$C_8H_{12}N_4S_2Br_2Zn$	$C_{12}H_{18}N_6S_3I_2Zn$	$C_8H_{12}N_4S_2Cl_2Cd$	$C_8H_{12}N_4S_2Br_2Cd$	$C_8H_{12}N_4S_2I_2Cd$
Formula weight	364.62	453.52	661.68	411.65	500.55	594.55
Crystal system	Orthorhombic	Orthorhombic	Orthorhombic	Monoclinic	Orthorhombic	Orthorhombic
Space group	$P2_12_12_1$ (#19)	$P2_12_12_1$ (#19)	$Pna2_1$ (#33)	$P2_1/a$ (#14)	$Pbcn$ (#60)	$Pca2_1$ (#29)
a (Å)	13.454(9)	13.706(6)	11.962(3)	19.785(6)	26.658(9)	11.542(6)
b (Å)	13.670(8)	14.021(7)	11.283(1)	7.710(3)	11.642(10)	14.138(5)
c (Å)	7.830(5)	7.809(2)	16.203(1)	9.612(3)	9.769(4)	9.926(3)
β (°)				96.77(2)		
V (Å^3)	1439(1)	1500(1)	2187(1)	1456(1)	3032(2)	1619(1)
Z	4	4	4	4	8	4
D_{calc} (g cm^{-3})	1.68	2.01	2.01	1.88	2.19	2.44
Crystal size (mm^3)	$0.44 \times 0.40 \times 0.34$	$0.60 \times 0.40 \times 0.15$	$0.40 \times 0.40 \times 0.20$	$0.50 \times 0.20 \times 0.17$	$0.50 \times 0.20 \times 0.17$	$0.35 \times 0.20 \times 0.10$
μ(Mo $K\alpha$) (cm^{-1})	23.49	72.40	42.42	21.38	69.90	54.08
$F000$	736	880	1264	808	1904	1096
Scan mode	ω–2θ	ω–2θ	ω–2θ	ω–2θ	ω	ω–2θ
Scan width (deg)	$1.63 \pm 0.30 \tan\theta$	$1.68 \pm 0.30 \tan\theta$	$1.63 \pm 0.30 \tan\theta$	$1.79 \pm 0.30 \tan\theta$	$1.21 \pm 0.30 \tan\theta$	$1.68 \pm 0.30 \tan\theta$
Scan speed (deg min^{-1})	12.0	10.0	10.0	8.00	10.0	8.00
Temp. (°C)	23	−53	23	23	−54	23
2θ range (deg)	5–55	5–55	5–55	5–55	5–55	5–55
Octant measured	$-h, +k, +l$	$-h, +k, +l$	$-h, -k, +l$	$+h, -k, \pm l$	$+h, +k, +l$	$+h, +k, +l$
Reflections collected	2001	2089	2990	3786	4118	2232
R_{int}	0.066	0.160	0.036	0.034	0.017	0.039
Unique reflections	1906	1984	2605	3333	3495	2047
No. of observations	1725 ($I > 2\sigma(I)$)	1806 ($I > 2\sigma(I)$)	2197 ($I > 2\sigma(I)$)	2848 ($I > 2\sigma(I)$)	2367 ($I > 2\sigma(I)$)	1960 ($I > 2\sigma(I)$)
No. of variables	154	154	217	154	144	154
Reflect./Para ratio	11.2	11.7	10.1	18.49	16.44	12.73
R^a	0.034	0.040	0.051	0.040	0.064	0.034
$R_w{}^a$	0.045	0.051	0.062	0.056	0.069	0.047
Good. of fit ind.	1.34	1.54	1.77	1.75	2.49	1.56
Max/Min peak (e Å^{-3})	0.63/−0.69	0.85/−0.69	0.61/−3.27	1.06/−1.59	1.16/−2.35	0.62/−1.30

[a] $R = \sum \| F_o| - |F_c| \| / \sum |F_o|$; $R_w = [(\sum w(|F_o| - |F_c|)^2 / \sum w F_o^2)]^{1/2}$, $w = 1/\sigma^2(|F_o|)$.

and **5** (−54 °C). All crystals were mounted on glass fiber by epoxy glue. The unit cell parameters of each crystal were obtained from a least-squares refinement based on 25 reflections ($20.5° < 2\theta < 30.0°$ (**1**), $25.5° < 2\theta < 30.0°$ (**2**), $25.0° < 2\theta < 30.0°$ (**3**), $25.0° < 2\theta < 28.5°$ (**4**), $22.0° < 2\theta < 27.0°$ (**5**), and $22.5° < 2\theta < 29.5°$ (**6**)). The intensity of three representative reflections monitored every 150 reflections did not show any decay in each complex. All data were corrected for Lorentz and polarization effect. The structures were solved by direct methods (SAPI 91) [26] and expanded using Fourier techniques [27]. The non-hydrogen atoms were refined anisotropically. An empirical absorption correction based on azimuthal scans of several reflections [28] (transmission factors ranging from 0.51 to 1.00 (**1**), from 0.37 to 1.00 (**3**), from 0.83 to 1.00 (**4**), from 0.70 to 1.00 (**5**)) or using the program DIFABS [29] (transmission factors ranging from 0.17 to 0.34 (**2**), from 0.28 to 0.42 (**6**)) was applied. Complex **5** contained two disordered ligand positions of equal occupancy. Therefore, isotropical refinements were applied to two imidazole ring atoms, and probable disorder of the S atom (S2) was not resolved at −54°C. Hydrogen atoms for all of the complexes were located on calculated positions. Refinement was carried out by a full matrix least-squares method on *F*. The absolute configuration was determined by Flack parameters (−0.01(1) for **1**, −0.02(1) for **2**, 0.12(8) for **3**, 0.10(7) for **6**) [30]. All calculations were performed using the teXsan [29] crystallographic software package of Molecular Structure Corporation.

3. Results and discussion

3.1. *Synthesis*

The neutral complexes $[MX_2(mitH)_2]$ (M = Zn; X = Cl (**1**), Br (**2**), M = Cd; X = Cl (**4**), Br (**5**), and I (**6**)) and cationic complex $[ZnI(mitH)_3]I$ (**3**) were readily prepared as white powders by the stoichiometric addition of a CH_3OH solution of metal(II) halogenide to a CH_3OH solution of the mitH ligand as shown in equation (2). Although the preparation method for **3** was the same as that for other complexes using ZnI_2 and mitH (equation (2)), the reaction product is $[ZnI(mitH)_3]I$. The expected complex $[ZnI_2(mitH)_2]$ is not obtained. Interestingly, when $[ZnBr_2(mitH)_2]$ (**2**) was recrystallized from a CH_3OH/H_2O mixed solvent, some yellow crystals were formed. The X-ray structures of these yellow crystals show that a disulfide bond was formed by the oxidation of S atoms in mitH ligands [31]. This seems to be the reason of the lower yield of **2** (29%) as colorless crystals.

$$\begin{aligned} &mitH + MX_2 \longrightarrow [MX_2(mitH)_2] \\ &\qquad\qquad M = Zn;\ X = Cl\ (\mathbf{1}),\ Br\ (\mathbf{2}) \\ &\qquad\qquad M = Cd;\ X = Cl\ (\mathbf{4}),\ Br\ (\mathbf{5}),\ I\ (\mathbf{6}) \\ &mitH + ZnI_2 \longrightarrow [ZnI(mitH)_3]I\ (\mathbf{3}) \end{aligned} \qquad (2)$$

UV-Vis absorption spectra in CH_3OH were measured. However, not only **1**, **2**, **4**–**6** but also **3** exhibit the same band at ca 259 nm, which is the same as that of free mitH. The spectra of the iodo complexes (**3** and **6**) show only another band (221 nm for **3** and 224 nm for **6**). These bands are expected to arise from CT transition(s) between iodide and metal(II) ions. Therefore, only mitH ligand would be dissociated

in solution, whereas the halide ions remain coordinated to the metal ion, such as $[MX_2]$. Consequently, we discuss here all the physicochemical properties in solid state.

3.2. *Crystal structures*

Representative structures of **1**–**6** are shown in figures 1–3. Selected bond distances and angles for all complexes are given in table 2. All of the metal(II) ions in the complexes

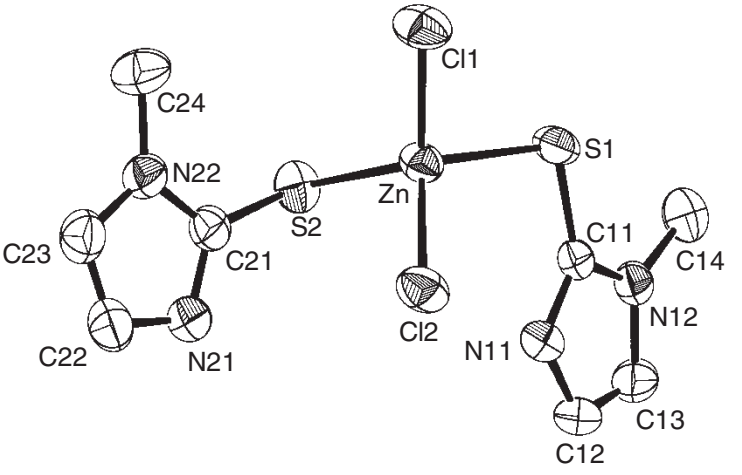

Figure 1. ORTEP diagram of $[ZnCl_2(mitH)_2]$ (**1**). Non-H atoms are represented with 50% probability ellipsoids.

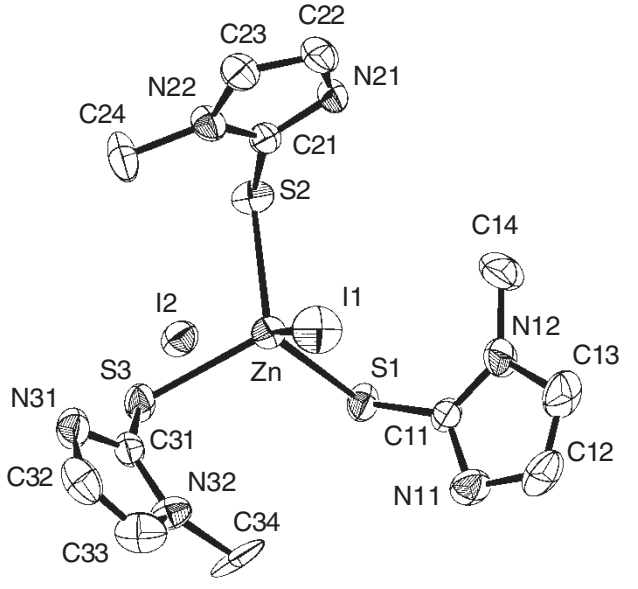

Figure 2. ORTEP diagram of $[ZnI(mitH)_3]I$ (**3**). Non-H atoms are represented with 50% probability ellipsoids.

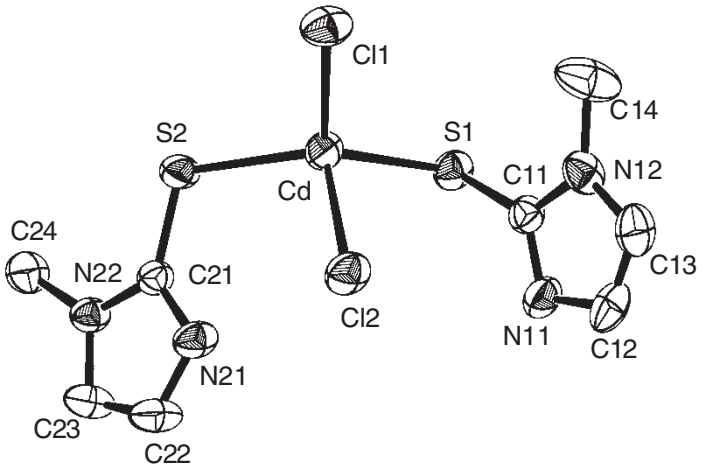

Figure 3. ORTEP diagram of $[CdCl_2(mitH)_2]$ (**4**). Non-H atoms are represented with 50% probability ellipsoids.

Table 2. Selected bond distances (Å) and angles (°) for complexes **1**–**6**.

	$[ZnCl_2(mitH)_2]$ (**1**)	$[ZnBr_2(mitH)_2]$ (**2**)	$[ZnI(mitH)_3]I$ (**3**)	$[CdCl_2(mitH)_2]$ (**4**)	$[CdBr_2(mitH)_2]$ (**5**)	$[CdI_2(mitH)_2]$ (**6**)
Bond distances						
M–X1	2.252(1)	2.390(1)	2.574(2)	2.426(1)	2.599(1)	2.785(1)
M–X2	2.259(1)	2.390(1)		2.501(1)	2.580(2)	2.778(1)
M–S1	2.336(2)	2.338(2)	2.376(3)	2.557(1)	2.534(3)	2.534(2)
M–S2	2.345(1)	2.342(2)	2.375(3)	2.529(1)	2.510(3)	2.565(2)
Zn–S3			2.373(3)			
S1–C11	1.709(4)	1.702(9)	1.71(1)	1.722(4)	1.708(9)	1.703(8)
S2–C21	1.714(5)	1.720(7)	1.71(1)	1.716(4)	1.95(2) C(21A) 1.87(1) C(21B)	1.715(9)
S(2)–C(31)			1.72(1)			
Bond angles						
S1–M–S2	103.83(5)	104.91(7)	105.6(1)	117.03(4)	107.00(9)	108.28(9)
S1–M–X1	102.54(5)	118.67(6)	112.98(8)	115.97(4)	111.75(8)	105.80(6)
S1–M–X2	115.39(5)	106.93(6)		98.75(4)	106.51(8)	113.94(6)
S2–M–X1	118.19(5)	101.28(6)	112.74(9)	111.32(4)	110.81(9)	104.72(6)
S2–M–X2	107.00(5)	115.77(6)		106.93(4)	110.21(8)	111.31(6)
X1–M–X2	110.07(5)	109.57(4)		104.76(4)	110.43(4)	112.21(4)
S3–Zn–I1			112.61(9)			
S1–Zn–S3			105.1(1)			
S2–Zn–S3			107.3(1)			
M–S1–C11	102.9(1)	99.8(2)	101.1(4)	102.4(1)	97.6(3)	109.1(3)
M–S2–C21	100.3(2)	103.3(2)	99.9(4)	107.8(1)	107.2(4) C(21A) 92.8(5) C(21B)	97.1(3)
Zn–S3–C31			100.7(4)			

except **3** occupy two-fold axes which bisect the S–M–S angles with the general formula $[MX_2(mitH)_2]$. Only **3** has a different structure (figure 2). Three mitH and one iodide ion coordinate to Zn(II) in **3**, and another iodide ion is present as a counter anion. The mitH ligands coordinate like a bowl, in which three imidazole rings stick out from the base formed by three S atoms. All complexes adopt a distorted tetrahedral

geometry with some deviations from an ideal angle of 109.5°. This geometry is typical for group 12 metal(II) complexes.

The S1–M–S2 angles in $[MCl_2(mitH)_2]$ increase from Zn(II) to Hg(II) (103.83(5)° for Zn(II) (**1**) < 117.03(4)° for Cd(II) (**4**) < 127.73(7)° for $[HgCl_2(mitH)_2]$), while the Cl1–M–Cl2 angles decrease (110.07(5)° for **1** > 104.76(4)° for **4** > 93.71(7)° for $[HgCl_2(mitH)_2]$) [21]. The average M–Cl distances increase from Zn(II) to Hg(II) ions (2.26 Å for **1** < 2.46 Å for **4** < 2.60 Å for $[HgCl_2(mitH)_2]$). However, the average M–S distance for **4** is longer than that for **1** and for the Hg(II) complex (2.34 Å for **1** < 2.54 Å for **4** > 2.45 Å for $[HgCl_2(mitH)_2]$). This difference may arise from lanthanide contraction, relativistic effects, and HSAB (hard soft acid base) principle [32, 33]. The same tendency is observed in a series of bromo and iodo complexes except **3** [21].

The C–S distances of all complexes are longer than those of free mitH ligand (1.685 Å) [34]. The value of π-character is very useful for discussing bonding of each complex [21]. The π-character of the C=S bond for the free ligand is calculated as 51.9%, using 1.82 Å as its C–S single bond distance [35]. The π-characters of the C=S bonds for all complexes are from 37.7% for **4** to 45.4% for **2**. Therefore, the C=S bonds become weaker by complexation. The M–S–C bond angles (from 97° to 109°), in which the S atom is sp^3 rather than sp^2, support also that the C=S bonds do not have a complete double bond. The main reason is that these mercaptoimidazole derivatives such as mitH are capable of existing in two tautomeric forms, thiol and thione, as shown in equation (1).

For the Cd(II) complexes **4**–**6** and the Hg(II) analogues [21], the X–M–X angles increase from the chloro complexes to the iodo ones due to the size of halide. Their S–M–S angles decrease from the chloro complexes to the iodo ones, because halide ions interfere sterically with the S atoms of the mitH ligands. The difference of X–Cd–X angles from the bromo complex **5** to iodo **6** increase only by ca 2° and there is little change in S–Cd–S angle. This suggests that Cd(II), mitH, and iodide ion are near the upper limit for CdX_2S_2 coordination mode. In addition, the I–M–I and S–M–S angles of $[MI_2(mitH)_2]$ (M = Cd and Hg) are almost the same, thus the maximum I–M–I and S–M–S angles in these complexes are expected to be 111–112° and 108–109° respectively. For the Zn(II) complexes, the differences of the X–Zn–X and S–Zn–S bond angles from chloro complex **1** to bromo **2** are little, that is to say, the combination of Zn(II) ion, mitH, and bromide ion is almost the upper limit for ZnX_2S_2 coordination. Therefore, **3** has a different, $ZnIS_3$, coordination mode.

3.3. *IR spectral behavior*

On the basis of X-ray structures, the stretching vibrations related to ligands and metal-ligand bonds can be assigned clearly. Most complexes with the mitH ligand are discussed in relation to the nature of C=S bond [16, 21, 22]. Selected IR data for "thioamide" bands (I–IV), which show the "thione" form in the free ligand and **1**–**6**, and ν(N–H) bands are summarized in Table 3. The ν(S–H) band at ca 2500 cm^{-1} is absent and the ν(N–H) band at ca 3100 cm^{-1} is present on complexation. All of the thioamide bands (I–IV) are shifted to some degree on complexation. The most significant change is observed in the thioamide band IV. This band has the largest proportion of ν(C=S) band activity and negative shift (15–60 cm^{-1}) in all complexes, suggesting that coordination occurs through the thione-S atom to the corresponding

Table 3. Major IR bands (cm^{-1}) and their assignments.

Complex	ν(N–H)	Thioamide bands[a]			
		I	II	III	IV
mitH	3158s, 3107vs, 3018m	1463vs	1274s	1091m	770s
$[ZnCl_2(mitH)_2]$ (**1**)	3251vs, 3179w, 3163w, 3151w, 3136m, 3044m	1478vs, 1467vs	1282m	1087m	732vs
$[ZnBr_2(mitH)_2]$ (**2**)	3204m, 3160w, 3130m	1475vs, 1458vs	1278m	1094m	741s
$[ZnI(mitH)_3]I$ (**3**)	3182m, 3119m	1457vs	1283s	1098s	757s
$[CdCl_2(mitH)_2]$ (**4**)	3173s, 3153s, 3117s, 3039m	1479s	1288m	1103m	754s, 729s
$[CdBr_2(mitH)_2]$ (**5**)	3245vs, 3123s, 3039w	1468vs	1287s	1101m	736vs
$[CdI_2(mitH)_2]$ (**6**)	3270vs, 3165s, 3124m, 3041w	1475vs, 1452s	1284m	1099m	731vs

[a]"Thioamide"-type modes are described as follows [22]; thioamide I = ν(C–N) + δ(CH); thioamide II = ν(C–N) + δ(CH) + ν(C=S); thioamide III = ν(C–N) + ν(C=S); thioamide IV = ν_s(C=S) + ν_{as}(C=S).

Table 4. Vibrational stretching bands (cm^{-1}) of complexes **1**–**6**.

Complex	Far-IR (Raman)	
	ν(M–S)	ν(M–X)
$[ZnCl_2(mitH)_2]$ (**1**)	320 (317)	290 (284)
$[ZnBr_2(mitH)_2]$ (**2**)	320 (314)	242 (253)
$[ZnI(mitH)_3]I$ (**3**)	304 (305)	–
$[CdCl_2(mitH)_2]$ (**4**)	306 (303)	271 (272)
$[CdBr_2(mitH)_2]$ (**5**)	306 (302)	229 (229)
$[CdI_2(mitH)_2]$ (**6**)	300 (292)	230 (228)
$[HgCl_2(mitH)_2]$ [21]	320	250

metal(II) ion. In addition, the ν(N–H) band displays positive shifts (30–100 cm^{-1}) [36], expected from a combination of factors including electronic changes within the molecule on complexation [36]. However, the shifts in **3** are smaller than those in **1** and **2**, reflecting the different structures.

3.4. *Far-IR and Raman spectral behavior*

The far-IR and Raman spectral data of all complexes are listed in table 4, together with the proposed assignments for the major bands. The assignments of these bands are carried out by comparison with the literature [25]. Since only the structure of $[HgCl_2(mitH)_2]$ was reported [21], we measured its far-IR spectrum and discuss ν(M–S) and ν(M–X) bands for all complexes.

Some absorption bands below 400 cm^{-1} are derived from newly formed bond(s) between the metal(II) ion and the donor atom(s) of the mitH ligand [25]. In addition, the bands of heavy donor atoms would appear at the lower energy side. Therefore, a new strong band at ca 300 cm^{-1}, which is found in the far-IR or Raman spectra of **1**–**6**, is assigned to ν(M–S). Another new band below 300 cm^{-1} is assigned to ν(M–X) band. The ν(M–S) band of the chloro complexes (**1** and **4**) shows a lower energy shift from 320 cm^{-1} for **1** to 306 cm^{-1} for **4** with increasing weight of metal(II) ions. However, ν(M–S) for the Hg(II) complex $[HgCl_2(mitH)_2]$ is found at 320 cm^{-1} similar to that for **1** and higher energy from that for **4** as shown in figure 4. These results

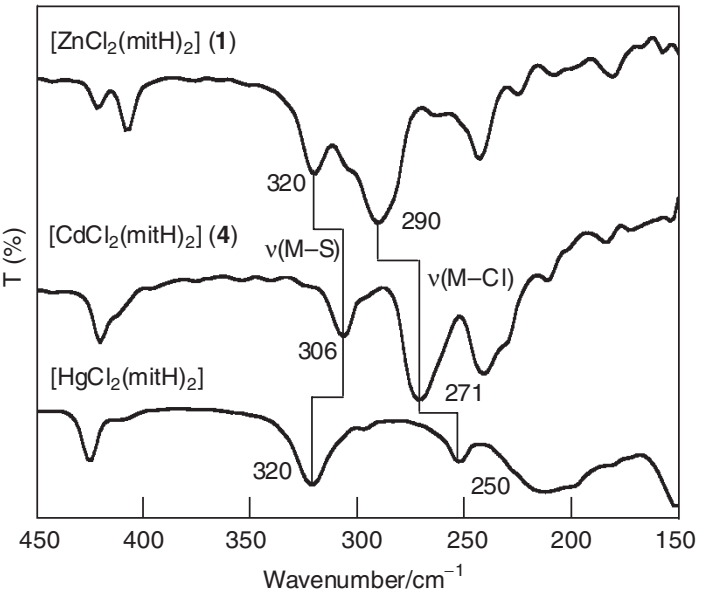

Figure 4. Far-IR spectra of $[MCl_2(mitH)_2]$ (M = Zn (**1**), Cd (**4**)) and $[HgCl_2(mitH)_2]$ [21].

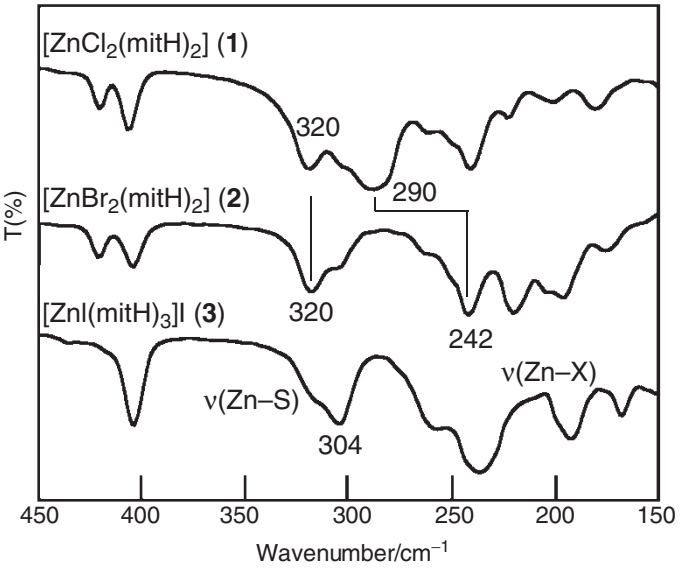

Figure 5. Far-IR spectra of $[ZnX_2(mitH)_2]$ (X = Cl (**1**), Br (**2**)) and $[ZnI(mitH)_3]I$ (**3**).

reflect the difference of M–S distances (vide supra). While the ν(M–X) bands show a lower energy shift with increasing weight of halide as shown in figures 5 and 6; 290 cm^{-1} for **1** > 242 cm^{-1} for **2**, 271 cm^{-1} for **4** > 229 cm^{-1} for **5** and 230 cm^{-1} for **6**. The ν(Cd–Br) band of **5** is difficult to assign, because it overlapped with other bands in the 220–250 cm^{-1} region. However, we assign the ν(Cd–Br) band at 229 cm^{-1}.

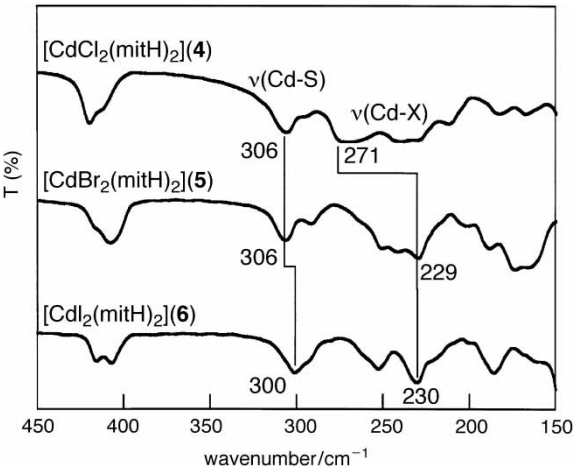

Figure 6. Far-IR spectra of $[CdX_2(mitH)_2]$ (X = Cl (**4**), Br (**5**), I (**6**)).

Table 5. Absorption spectral (solid) data (nm) of complexes **1**–**6**.

Complex	CT band	CT bands	Other bands
$[ZnCl_2(mitH)_2]$ (**1**)	275	–	215(sh)
$[ZnBr_2(mitH)_2]$ (**2**)	277	206	–
$[ZnI(mitH)_3]I$ (**3**)	281	216, 229(sh)	
$[CdCl_2(mitH)_2]$ (**4**)	287	207	–
$[CdBr_2(mitH)_2]$ (**5**)	290	220	–
$[CdI_2(mitH)_2]$ (**6**)	293	227	264

Accordingly, these results also support the assignment of ν(M–X) bands reflecting the difference of M–X distances. The far-IR spectrum of **3** shows some new bands as shown in figure 5. The band at 304 cm^{-1} is assigned to ν(Zn–S) band, but assignment of ν(Zn–I) bands is difficult. The Raman bands of all complexes are little shifted in comparison with the far-IR bands. That is a common result for C_{2v} point group, and predictable from calculation of vibration mode for C_2 point group [37].

3.5. *UV-Vis spectral behavior*

The UV-Vis spectral results in solid state for **1**–**6** are summarized in table 5. In solid state, the Cd(II) complexes **4**–**6** show more than two bands as shown in figure 7. The absorption bands shift to lower energy from chloro to iodo Cd(II) complexes (207 nm for **4** < 220 nm for **5** < 227, 264 nm for **6**). The Zn(II) complexes **1** and **2** show one band in the 200–220 nm region as shoulder or small peak. The free mitH ligand has absorption bands at 246(sh), 274(sh), and 294 nm. These results suggest that the absorption bands in the 200–230 nm region arise from CT transition between halide and metal(II) ions.

The absorption bands at 230–300 nm are assigned to an S-to-Cd(II) CT transition, when one or more S atoms bind to Cd(II) ion [10]. Spiro and co-workers reported that S-to-Cd(II) CT transition appears at 238 nm for binding two cysteine and

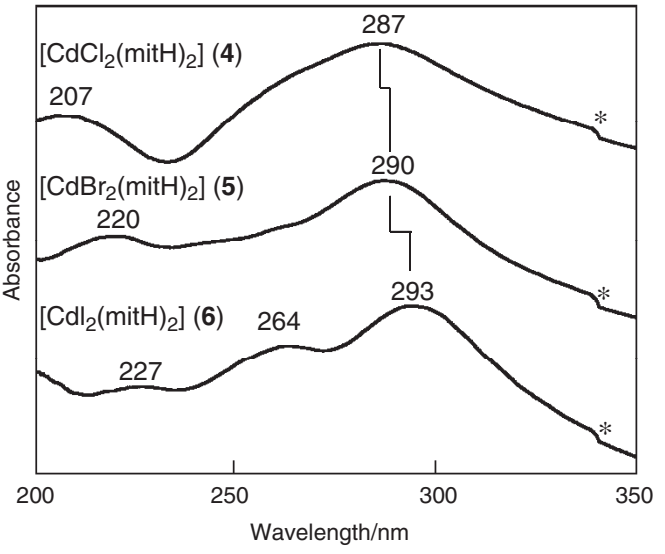

Figure 7. UV-Vis absorption spectra (solid state) of $[CdX_2(mitH)_2]$ (X = Cl (**4**), Br (**5**), I (**6**)). *: Artifact.

two histidine residues in Cd(II) substituted zinc-finger peptides [38]. Cd(II) ion is used in place of Zn(II) ion, because S-to-Cd(II) CT transition bands are stronger and are found at lower energy than those of Zn(II). For the chloro complexes **1** and **4** and the bromo complexes **2** and **5**, the absorption bands in the 270–300 nm region are shifted to lower energy from the Zn(II) complexes to the Cd(II) complexes (275 nm for **1** < 287 nm for **4**, 277 nm for **2** < 290 nm for **5**). Therefore, the bands in the 270–300 nm region are assignable to S-to-M(II) CT bands. Complex **3** shows some absorption bands at 216, 229(sh), and 281 nm. Similar to other complexes, the band at 281 nm is assigned to the S-to-Zn(II) CT transition. Either one or both bands at 216 and 229(sh) nm are expected to arise from CT between iodide ion and Zn(II) ion.

4. Conclusions

The Zn(II) and Cd(II) complexes with mitH were synthesized systematically for assignments of coordination modes of group 12 metal(II) complexes. Structures of all complexes except for **3** were determined as an MX_2S_2 type structure by X-ray analysis. Complex **3** has the ZnS_3I type structure which is favorable to take a tetrahedral configuration with Zn(II) ion, iodide ion, and mitH ligands. These results indicate that their stretching vibration frequencies and their energies of CT transition bands are useful signals for determining metal coordination sphere in group 12 metal(II) complexes. These spectroscopic techniques could be extended to assign some proteins containing group 12 metal(II) ions in their active sites.

Supplementary material

Tables of atomic coordinates, anisotropic thermal parameters, bond distances and angles, and torsion angles of **1**–**6** are available from the authors upon request.

Crystallographic data have been deposited at the Cambridge Crystallographic Data Centre, CCDC Nos. numbers 220844-220849 for compounds **1**–**6**. Copies of the data can be obtained free of charge on application to the Director CCDC, 12 Union Road, Cambridge CB2 1EZ, UK (fax: +44-1223-336-033; e-mail deposit@ccdc.ac.uk or www: http://www.ccdc.cam.ac.uk).

Acknowledgements

We thank Professor K. Tanaka of Institute of Molecular Science for FT-Raman measurements and Dr. M. Yamazaki of Rigaku Corporation for determining molecular structure of **3**. This research was supported in part by Grant-in-Aid for Scientific Research (Nos. 11640555, 13555257, and 14540510) and the 21st Century COE program from the Japan Society for the Promotion of Science.

References

[1] R.H. Holm, P. Kennepohl, E.I. Solomon. *Chem. Rev.*, **96**, 2239 (1996).
[2] R. Baggio, M.T. Garland, M. Perec. *J. Chem. Soc., Dalton Trans.*, 3367 (1993).
[3] R. Burth, H. Vahrenkamp. *Inorg. Chim. Acta*, **282**, 193 (1998).
[4] J.J. Wilker, S.J. Lippard. *J. Am. Chem. Soc.*, **117**, 8682 (1995).
[5] D.T. Corwin Jr, S.A. Koch. *Inorg. Chem.*, **27**, 493 (1988).
[6] W.-Y. Sun, L. Zhang, K.-B. Yu. *J. Chem. Soc., Dalton Trans.*, 795 (1999).
[7] S.J. Lippard, J.M. Berg. *Principles of Bioinorganic Chemistry*, University Science Books, Mill Valley (1994).
[8] J.A. Cowan. *Inorganic Biochemistry: An Introduction*, 2nd Edn, VCH Publishers, Inc., New York (1996).
[9] M.J. Stillman, C.F. Shaw III, K.T. Suzuki (Eds), *METALLOTHIONEINS: Synthesis, Structure and Properties of Metallothioneins, Phytochelatins and Metal-Thiolate Complexes*, VCH Publishers, Inc., New York (1992).
[10] G. Fleissner, P.M. Kozlowski, M. Vargek, J.W. Bryson, T.V. O'Halloran, T.G. Spiro. *Inorg. Chem.*, **38**, 3523 (1999).
[11] S.P. Watton, J.G. Wright, F.M. MacDonnell, J.W. Bryson, M. Sabat, T.V. O'Halloran. *J. Am. Chem. Soc.*, **112**, 2824 (1990).
[12] G. Fleissner, M.D. Reigle, T.V. O'Halloran, T.G. Spiro. *J. Am. Chem. Soc.*, **120**, 12690 (1998).
[13] E.S. Raper, I.W. Nowell. *Acta Crystallogr., Sect. B*, **35**, 1600 (1979).
[14] E.S. Raper, I.W. Nowell. *Inorg. Chim. Acta*, **43**, 165 (1980).
[15] E.S. Raper, M.E. O'Neill, J.A. Daniels. *Inorg. Chim. Acta*. **41**, 145 (1980).
[16] J.R. Creighton, D.J. Gardiner, A.C. Gorvin, C. Gutteridge, A.R.W. Jackson, E.S. Raper, P.M.A. Sherwood. *Inorg. Chim. Acta*, **103**, 195 (1985).
[17] E.S. Raper, W. Clegg. *Inorg. Chim. Acta*, **180**, 239 (1991).
[18] E.S. Raper, J.R. Creighton, W. Clegg. *Inorg. Chim. Acta*, **183**, 179 (1991).
[19] I.W. Nowell, A.G. Cox, E.S. Raper. *Acta Crystallogr., Sect. B*, **35**, 3047 (1979).
[20] D.A. Cooper, S.J. Rettig, A. Storr, J. Trotter. *Can. J. Chem.*, **64**, 1643 (1986).
[21] N.A. Bell, T.N. Branston, W. Clegg, J.R. Creighton, L. Cucurull-Sánchez, M.R.J. Elsegood, E.S. Raper. *Inorg. Chim. Acta*, **303**, 220 (2000).
[22] Z. Popovic, D. Matkovic-Calogovic, Z. Soldin, G. Pavlovic, N. Davidovic, D. Vikic-Topic. *Inorg. Chim. Acta*, **294**, 35 (1999).
[23] N.A. Bell, W. Clegg, J.R. Creighton, E.S. Raper. *Inorg. Chim. Acta*, **303**, 12 (2000).
[24] E.S. Raper, J.R. Creighton, N.A. Bell, W. Clegg, L. Cucurull-Sánchez. *Inorg. Chim. Acta*, **277**, 14 (1998).
[25] R. Shunmugam, D.N. Sathyanarayana. *J. Coord. Chem.*, **12**, 151 (1983).
[26] SAPI 91: H.-F. Fan. *Structure Analysis Programs with Intelligent Control*, Rigaku Corporation, Tokyo, Japan (1991).
[27] DIRDIF 94: P.T. Beurskens, G. Admiraal, G. Beurskens, W.P. Bosman, R. de Gelder, R. Israel, J.M.M. Smits. *The DIRDIF-94 Program System*, Technical Report of the Crystallography Laboratory, University of Nijmegen, The Netherlands (1994).
[28] teXsan: *Single Crystal Structure Analysis Package, Version. 1.10b*, Molecular Structure Corporation, The Woodlands, TX (1999).
[29] N. Walker, D. Stuart. *Acta Crystallogr., Sect. A*, **39**, 158 (1983).

[30] H.D. Flack. *Acta Crystallogr., Sect. A.*, **39**, 876 (1983).
[31] Unpublished data; Zinc center in the yellow crystal has a ZnN_2Br_2 tetrahedral structure which binds to two bromide ions and two nitrogen atoms of mitH, in which S atoms formed disulfide bond. Recently disulfide molecule (bis[1-methylimidazole(2)]disulfide) has been reported: M.C. Aragoni, M. Arca, F. Demartin, F.A. Devillanova, A. Garau, F. Isaia, V. Lippolis and G. Verani. *J. Am. Chem. Soc.* **124**, 4538 (2002).
[32] F.A. Cotton, G. Wilkinson, C.A. Murillo, M. Bochmann. *Advanced Inorganic Chemistry*, 6th Edn. John Wiley & Sons, Inc, New York (1999).
[33] J.E. Huheey, E.A. Keiter, R.L. Keiter. *Inorganic Chemistry*, 4th Edn, Harper Collins College Publishers, New York (1993).
[34] E.S. Raper, J.R. Creighton, R.E. Oughtred, I.W. Nowell. *Acta Crystallogr., Sect. B*, **39**, 355 (1983).
[35] N. Trinajstic. *Tetrahedron Lett.*, **12**, 1529 (1968).
[36] E.S. Raper, H. Crackett. *Inorg. Chim. Acta*, **50**, 159 (1981).
[37] K. Nakamoto. *Infrared and Raman Spectra of Inorganic and Coordination Compounds*, 5th Edn, John Wiley and Sons, New York (1997).
[38] M. Vargek, X. Zhao, Z. Lai, G.L. McLendon, T.G. Spiro. *Inorg. Chem.*, **38**, 1372 (1999).